Dominant-Negative but not Gain-of-Function Effects of a *p53.R270H* Mutation in Mouse Epithelium Tissue after DNA Damage

Susan W.P. Wijnhoven,[1] Ewoud N. Speksnijder,[1] Xiaoling Liu,[2] Edwin Zwart,[1] Conny Th. M. vanOostrom,[1] Rudolf B. Beems,[1] Esther M. Hoogervorst,[1] Mirjam M. Schaap,[1] Laura D. Attardi,[3] Tyler Jacks,[4] Harry van Steeg,[1] Jos Jonkers,[2] and Annemieke de Vries[1]

[1]Laboratory of Toxicology, Pathology and Genetics, National Institute of Public Health and the Environment, Bilthoven, the Netherlands; [2]Division of Molecular Biology, Netherlands Cancer Institute, Amsterdam, the Netherlands; [3]Division of Radiation and Cancer Biology, Department of Radiation Oncology, Department of Genetics, Stanford University School of Medicine, Stanford, California; and [4]Center for Cancer Research, Massachusetts Institute of Technology, Cambridge, Massachusetts

Abstract

***p53* alterations in human tumors often involve missense mutations that may confer dominant-negative or gain-of-function properties. Dominant-negative effects result in inactivation of wild-type p53 protein in heterozygous mutant cells and as such in a p53 null phenotype. Gain-of-function effects can directly promote tumor development or metastasis through antiapoptotic mechanisms or transcriptional activation of (onco)genes. Here, we show, using conditional mouse technology, that epithelium-specific heterozygous expression of mutant p53 (i.e., the *p53.R270H* mutation that is equivalent to the human hotspot R273H) results in an increased incidence of spontaneous and UVB-induced skin tumors. Expression of *p53.R270H* exerted dominant-negative effects on latency, multiplicity, and progression status of UVB-induced but not spontaneous tumors. Surprisingly, gain-of-function properties of *p53.R270H* were not detected in skin epithelium. Apparently, dominant-negative and gain-of-function effects of mutant p53 are highly tissue specific and become most manifest upon stabilization of p53 after DNA damage.** [Cancer Res 2007;67(10):4648–56]

Introduction

p53 is the most extensively studied tumor suppressor gene, encoding a transcriptional regulator that controls cell cycle progression and apoptosis (1). In unstressed cells, p53 is present in a latent form and is maintained at low levels through targeted degradation. In response to DNA damage or cellular stress, its activity increases to exert its function as a transcription factor (2), resulting in a cascade of events that eventually prevent tumor development. The *p53* gene is altered in more than 50% of spontaneous tumors in humans, and germ-line *p53* mutations confer cancer predisposition to individuals with Li-Fraumeni syndrome (3, 4).

In contrast to modifications found in other tumor suppressors, which are typically deleted, truncated, silenced, or otherwise down-regulated in many cancers, the majority of *p53* alterations are missense mutations in the DNA binding domain, disrupting the ability of the protein to bind DNA and activate transcription (5–7). Loss of the remaining wild-type allele frequently occurs in a later stage of tumor development. Functional consequences of missense mutations compared with deletions of *p53* have been extensively studied *in vitro* (ref. 8 and references therein). *p53* missense mutations are commonly loss-of-function mutations that mimic absence of p53, because mutant p53 is no longer able to inhibit cell cycling or induce apoptosis. In addition, these missense mutations are thought to have dominant-negative and/or gain-of-function characteristics (8–10). Dominant-negative p53 mutants can inhibit the function of wild-type p53 through protein-protein interactions (11), whereas gain-of-function mutants have additional functions not seen in wild-type p53 (12). However, the majority of studies describing these mutant p53 characteristics are based on *in vitro* overexpression analyses.

The first *in vivo* studies to determine the fundamental role of *p53* as a tumor suppressor were done in mice with heterozygous or homozygous deletions of *p53* (13–15). To more accurately mimic LFS and examine the effect of (specific) *p53* missense mutations on tumorigenesis *in vivo*, transgenic strains were produced, which overexpress mutant *p53* (16–20). Collectively, studies with these transgenic models show that mutant *p53* overexpression results in accelerated spontaneous and carcinogen-induced tumorigenesis, with a dominant-negative effect of the mutant protein (16). To more physiologically model LFS in mice and investigate the potential dominant-negative or gain-of-function effects by mutant p53 *in vivo*, (conditional) mutant *p53* knock-in mice carrying targeted mutations in the endogenous *p53* gene locus were recently generated (21, 22). One *p53* mutant mouse strain was generated with an arginine to histidine mutation at codon 172, corresponding to the *p53.R175H* hotspot mutation that destroys the structural integrity of the p53 protein (21, 22). A second strain was engineered to carry an arginine to histidine mutation at *p53* codon 270 (22), which corresponds to the *p53.R273H* hotspot mutation frequently found in human cancers and replaces an arginine that directly contacts DNA. The phenotypes of these mutant mice indicate clear gain-of-function properties of mutant *p53*, with a metastatic tumor phenotype as the most striking difference between missense mutant mice and *p53*-null mice. Furthermore, tumor spectra changed, with an overall increase in the incidence of carcinomas and B-cell lymphomas in $p53^{R270H/+}$ mice and osteosarcomas in $p53^{R172H/+}$ mice (22).

Note: Supplementary data for this article are available at Cancer Research Online (http://cancerres.aacrjournals.org/).

Requests for reprints: Annemieke de Vries, Laboratory of Toxicology, Pathology and Genetics, National Institute of Public Health and the Environment, P.O. Box 1, 3720 BA Bilthoven, the Netherlands. Phone: 31-30-2743483; Fax: 31-30-2744446; E-mail: Annemieke.de.Vries@RIVM.nl.

doi:10.1158/0008-5472.CAN-06-4681

However, the above-described studies focused on effects of constitutive expression of the *p53* point mutants in all tissues (21, 22). One of the strengths of conditional mouse technology is the potential for tissue-specific analyses of the adverse effects of gene alterations using transgenic mice with tissue- and cell-specific Cre expression. Because it is well known (6, 23, 24) that the tumorigenic potential of individual mutant p53 proteins can vary between cell types and tissues, it would be important to analyze the effect of such mutant proteins exclusively in a tissue or cell type of interest. Furthermore, tissue-specific analysis can be preferred to investigate the effect of carcinogen exposure. We and others have previously studied the tissue-specific effects of the *p53* missense mutation at codon 270 in mammary gland and lung epithelium, respectively (25, 26). Both models mimic human tumor development and, as such, are suitable to study and develop better treatment strategies for breast and lung cancer patients, respectively.

Here, we analyze whether the *p53.R270H* mutation has dominant-negative and/or gain-of-function properties in mouse skin epithelium, either unchallenged or challenged by DNA damage–inducing chronic UVB exposure. Nonmelanoma skin cancer is currently the most common type of human cancer, and its incidence is increasing at an astonishing rate (27). *p53* is found mutated in 50% of skin cancers overall and up to 90% of squamous cell carcinoma (SCC) specifically (28). Interestingly, in the vast majority of these tumors, the remaining wild-type *p53* allele is intact rather than lost through loss of heterozygosity (LOH) as frequently observed in other tumor types (14, 29). This might indicate that the heterozygous presence of a *p53* mutation is sufficient to trigger skin tumor development. Here, heterozygous $p53^{LSL\text{-}R270H/+}$ mice were crossed with K14*cre* transgenic mice, resulting in epithelium-specific expression of the mutant p53.R270H protein. Skin tumor development and acute cellular responses after UVB exposure were subsequently compared with those in conditional heterozygous and homozygous *p53* knockout mice as controls. In this way, a clean skin-specific comparison of effects can be made between *p53* missense and *p53* null mutations. We show here that, especially after UVB-induced DNA damage, a *p53.R270H* mutation shows dominant-negative but not gain-of-function activities in skin tumor development.

Materials and Methods

Mice and Genotyping

Cloning of the $p53^{LSL\text{-}R270H}$ targeting vector, homologous recombination experiments in embryonic stem cells, and generation of conditional $p53^{LSL\text{-}R270H}$ mice were described elsewhere (22, 30). Genotyping of $p53^{LSL\text{-}R270H}$ mice was done by a PCR/digestion–based assay as described previously (25).

K14*cre* mice expressing Cre-recombinase under control of a human K14 gene promoter were used to induce *Cre*-mediated deletion of the floxed stop-cassette specifically in dividing cells of stratified epithelia (31). The presence of Cre-recombinase was determined by PCR as described before (25).

The presence of a $p53^{F2\text{-}10}$ allele in *p53* conditional knockout mice and a deletion of exons 2 to 10 in *p53* ($p53^{\Delta 2\text{-}10}$ allele) were detected as described earlier (31).

To obtain homozygous hairless mice of all genotypes, all strains were crossed twice to hairless SKH1 mice (Charles River). Animals in experiment were obtained from crossing these hairless *p53* mutant and/or *p53* conditional knockout mice to hairless K14*cre* mice.

Analysis of Spontaneous and UVB-Induced (Skin) Tumor Development

Spontaneous tumor development was determined in groups of six female and two male mice of the following genotypes: K14*cre*;$p53^{+/+}$, K14*cre*;$p53^{LSL\text{-}R270H/+}$, K14*cre*;$p53^{F2\text{-}10/+}$, K14*cre*;$p53^{F2\text{-}10/F2\text{-}10}$, and K14*cre*;$p53^{LSL\text{-}R270H/F2\text{-}10}$. For UVB experiments, groups of 14 mice of the same genotypes, all consisting of 50% females and 50% males, were irradiated daily with a dose of 600 J/m^2 UVB using Philips TL12 lamps, starting at the age of 6 weeks. All mice were checked weekly for the development of tumors until a maximum age of 78 weeks. Mice carrying tumors ≥4 mm in size or ≥15 small tumors were sacrificed. Control tissues and a maximum of six skin tumors were collected and processed for histopathology and DNA/RNA isolation following standard procedures.

Short-Term UVB Exposure

For determination of the maximum tolerated dose (MTD), two mice of each genotype were exposed to daily doses of UVB of 0, 500, 750, 1,000, or 1,250 J/m^2 during seven subsequent days and checked for erythema and other acute effects. For determination of apoptotic/sunburn cells, two mice per genotype were exposed to a single dose of 500 and 1,000 J/m^2. Front and back skin were isolated together with control tissue 24 h after the UVB exposure and processed for histopathology and DNA/RNA isolation following standard procedures.

Molecular Analysis of Tumors and Tissues

Expression of the R270H point mutation or deletion of exons 2 to 10 of *p53*. Analysis of *in vivo* expression of the *p53.R270H* mutant allele in skins, control tissue (spleen), and tumors was done as described earlier (25). Deletion of the conditional $p53^{F2\text{-}10}$ allele in skin (tumors) was determined by PCR as described for mouse genotyping above.

Determination of loss of the wild-type *p53* allele (LOH) and additional *p53* gene mutations in skin tumors. LOH was detected by reverse transcription-PCR (RT-PCR) as described previously (25). Frozen skin tumors of UVB-exposed mice were analyzed for acquired *p53* mutations by direct sequencing as described earlier (32).

Histology and Immunohistochemistry

Collected tissues and tumors from short-term and long-term UV studies were preserved in a neutral aqueous phosphate-buffered 4% solution of formaldehyde (10% neutral buffered formalin). The tissues were embedded in paraffin wax, sectioned at 5 μm, and stained with H&E for histopathologic evaluation.

Immunohistochemistry of skin sections from short-term UV studies. Isolated skin samples from short-term UV studies were stained with the following antibodies: caspase-3 (Asp^{175}, 1:200; Cell Signaling), Bax (P19, 1:50; Santa Cruz Biotechnology), Puma (Puma, 1:2,000; Cell Signaling), and Perp (33). All stainings (except for Perp) were done as described earlier (34) using a secondary goat anti-rabbit/biotin antibody (Vector Laboratories) and subsequently a streptavidin-complex peroxidase Elite kit (Vector Laboratories). For antigen retrieval, deparaffinized tissue sections were heated for 30 min in a 10 mmol/L citrate buffer (pH 6.0) at 95°C. Perp staining was done as reported previously (33).

Immunohistochemistry of skin tumors from long-term UV studies. Four tumors per genotype were analyzed for the expression of the oncogenes *cyclin D1* and *H-Ras*. Antibodies used were the rabbit monoclonal antibody SP4 for cyclin D1 (1:200; GeneTex, Inc.) and F235 for H-Ras (1:2,000; Santa Cruz Biotechnology). The staining protocol for cyclin D1 was identical to the protocols described in the previous section. For H-Ras stainings, a secondary donkey anti-mouse/biotin antibody (Jackson ImmunoResearch) was used.

Statistical Analysis

Statistical analyses of tumor-free survival curves included calculation of Kaplan-Meier distributions of survival of two different treatment groups and comparison by a two-sided log-rank test (SPSS, version 11). Multiplicity of tumors was statistically analyzed by an unpaired *t* test. $P < 0.05$ was taken as significant.

Results

Skin-specific *p53.R270H* expression and *p53.F2-10* deletion. To assess whether the introduction of K14*cre* leads to epithelial-specific removal of the transcriptional stop-cassette and subsequent

expression of the p53.R270H mutant protein, we determined expression of the mutation in skin and control tissue of young K14*cre;p53*$^{LSL\text{-}R270H/+}$ mice by RT-PCR. As is clear from Fig. 1*A*, the *p53.R270H* mutation is expressed in skins of young adult K14*cre;p53*$^{LSL\text{-}R270H/+}$ mice. As expected, in non-epithelium tissue (i.e., spleen) of the same mice, only the wild-type allele was detectable. K14*cre*-induced recombination of the *p53*$^{F2\text{-}10}$ allele in skin of young adult homozygous and heterozygous conditional *p53* knockout mice was very efficient as all skin samples tested showed a recombined *p53*$^{F2\text{-}10}$ allele (Fig. 1*B*).

Survival and spontaneous skin tumor development in K14*cre;p53*$^{LSL\text{-}R270H/+}$ mice. To examine a potential dominant-negative and/or gain-of-function effect of the *p53.R270H* mutation on spontaneous tumorigenesis of epithelial cell origin, both female and male K14*cre;p53*$^{+/+}$, K14*cre;p53*$^{LSL\text{-}R270H/+}$, K14*cre;p53*$^{F2\text{-}10/+}$, K14*cre;p53*$^{F2\text{-}10/F2\text{-}10}$, and K14*cre;p53*$^{LSL\text{-}R270H/F2\text{-}10}$ in a hairless background were followed as they aged for the development of spontaneous tumors. All genotypes analyzed seem susceptible for spontaneous tumor development, especially in the skin (Fig. 2*A*). Large differences in tumor latency times occur when functional p53 is (partly) lacking, as significantly reduced tumor latencies are observed in both heterozygous K14*cre;p53*$^{LSL\text{-}R270H/+}$ and K14*cre;p53*$^{F2\text{-}10/+}$ mice when compared with K14*cre;p53*$^{+/+}$ littermates (P = 0.0013 and 0.0011, respectively; Fig. 2*B*). However, no difference in tumor latency time could be observed between heterozygous K14*cre;p53*$^{LSL\text{-}R270H/+}$ and K14*cre;p53*$^{F2\text{-}10/+}$ mice (P = 0.8645), pointing to the absence of a dominant-negative effect of the *p53.R270H* mutation in epithelium cells during spontaneous (skin) tumor development. In contrast, a clear *p53* gene dosage effect was present, as homozygous K14*cre;p53*$^{F2\text{-}10/F2\text{-}10}$ mice show a significantly accelerated (skin) tumor development when compared with heterozygous K14*cre;p53*$^{F2\text{-}10/+}$ (P = 0.0002) and K14*cre;p53*$^{LSL\text{-}R270H/+}$ mice (P = 0.0002). Spontaneous tumor-free survival curves of K14*cre;p53*$^{LSL\text{-}R270H/F2\text{-}10}$ and K14*cre;p53*$^{F2\text{-}10/F2\text{-}10}$ mice seem identical, indicating that in this K14*cre* mouse model, a gain-of-function effect of the p53.R270H mutant protein is absent during spontaneous tumor development. The majority of tumors develop in the skin, but also epithelial mammary tumors were found as reported earlier after recombination of conditional *p53*

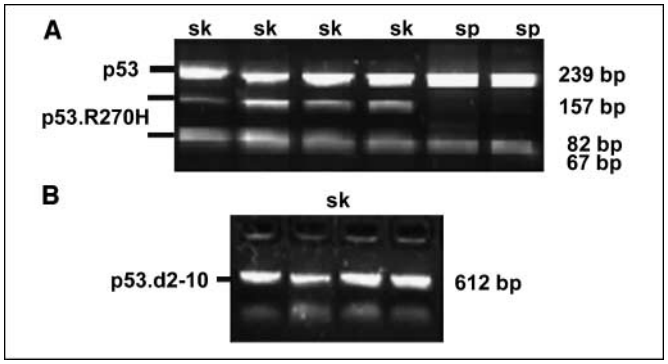

Figure 1. Molecular characterization of epithelial-specific *p53.R270H* expression and recombination of exons 2 to 10. *A,* RT-PCR analysis followed by *Nla*III digestion to determine *p53.R270H* expression in different tissues of young adult K14*cre;p53*$^{LSL\text{-}R270H/+}$ mice. Expression of the R270H point mutation in *p53* was determined in the obtained PCR product of 333 bp. *Nla*III digestion of wild-type *p53* resulted in four products of 239, 67, 18, and 9 bp, whereas in the presence of *R270H*-mutated *p53*, five products are generated (157, 82, 67, 18, and 9 bp). *Lanes 1* to *4,* digestion products from skins (*sk*) isolated from four individual mice, showing expression of mutant *p53. Lanes 5* and *6,* only wild-type *p53* is detectable in spleens (*sp*) of two different mice. Only digestion products ≥ 67 bp are visible (products of 67 and 82 bp comigrate). *B,* PCR analysis on genomic DNA to determine the recombination of exons 2 to 10 in skin samples of four individual young adult K14*cre;p53*$^{F2\text{-}10/+}$ mice. All lanes clearly show the 612-bp deletion PCR product obtained by the combination of the forward primer in intron 1 and the reverse primer in intron 10 (31).

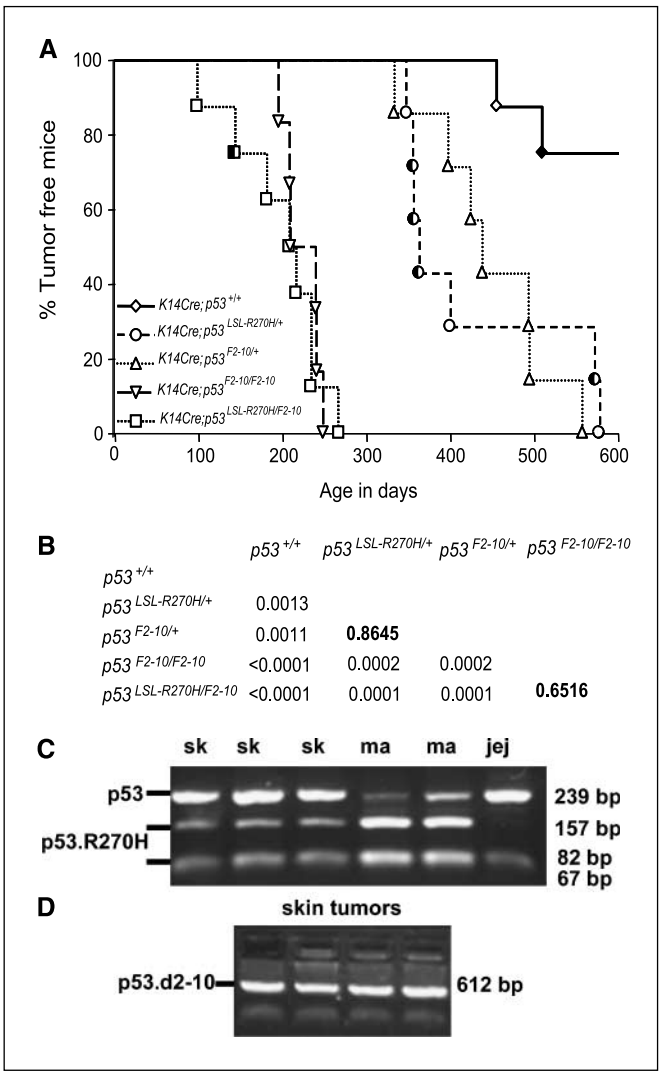

Figure 2. Spontaneous tumor development in *p53*-defective K14*cre* mice. Effect of expression of the R270H mutation and/or deletion of exons 2 to 10 in *p53* on spontaneous (skin) tumor development. *A,* tumor-free survival curves of untreated K14*cre;p53*$^{+/+}$, K14*cre;p53*$^{LSL\text{-}R270H/+}$, K14*cre;p53*$^{F2\text{-}10/+}$, K14*cre;p53*$^{F2\text{-}10/F2\text{-}10}$, and K14*cre;p53*$^{LSL\text{-}R270H/F2\text{-}10}$ in a hairless background. Tumor types were classified as skin tumors (*open symbols*) and other tumors (*filled symbols*). Other tumors included a hepatocellular adenoma (in liver of *p53*$^{+/+}$ male after 485 d), two adenocarcinomas of the mammary gland (in two individual *p53*$^{R270H/+}$ females after 349 d), one hemangiosarcoma (in intestine of a K14*cre;p53*$^{LSL\text{-}R270H/+}$ female after 356 d), and two lymphomas (one in jejunum of a K14*cre;p53*$^{LSL\text{-}R270H/+}$ male after 579 d and one in a K14*cre;p53*$^{LSL\text{-}R270H/F2\text{-}10}$ female after 186 d). *B,* schematic overview of *P* values of the statistical analyses of spontaneous tumor-free survival curves analyzed by calculation of Kaplan-Meier distributions of survival and comparison by a two-sided log-rank test. With a level of significance of $P \leq 0.05$, no statistically significant difference in spontaneous skin tumor latency time is observed between K14*cre;p53*$^{LSL\text{-}R270H/+}$ and K14*cre;p53*$^{F2\text{-}10/+}$ mice or between K14*cre;p53*$^{LSL\text{-}R270H/F2\text{-}10}$ and K14*cre;p53*$^{F2\text{-}10/F2\text{-}10}$ mice. *C,* analysis of R270H expression in different tumor types in unexposed K14*cre;p53*$^{LSL\text{-}R270H/+}$ mice. *Lanes 1* to *5, Nla*III digestion products of both wild-type *p53* and R270H mutated *p53* in three skin (*sk*) and two mammary gland (*ma*) tumors. The lymphoma arisen in jejunum (*jej*) in lane 6 showed only wild-type *Nla*III digestion products of *p53. D,* PCR analysis in skin tumors of unexposed K14*cre;p53*$^{F2\text{-}10/+}$ mice. All lanes clearly show the 612-bp deletion PCR product obtained by the combination of the forward primer in intron 1 and the reverse primer in intron 10 (31).

and *Brca* alleles with K14*cre* (31). Here, mammary tumors were only found in K14*cre;p53*$^{LSL\text{-}R270H/+}$ mice, similar to results reported recently in a mammary gland–specific *WAPCre* background (25). Molecular analysis of skin tumors as well as mammary tumors clearly showed *p53.R270H* expression that was absent in a lymphoma in the jejunum (Fig. 2*C*), confirming epithelium-specific expression of mutant p53. In line with this, deletion of exons 2 to 10 in K14*cre;p53*$^{F2\text{-}10/+}$ mice was visible in all skin tumors analyzed (Fig. 2*D*).

UVB-induced skin tumor development in *p53*-defective mice. The effect of the *p53.R270H* hotspot mutation on the tumor suppressive activity of p53 after DNA damage was subsequently investigated by exposure of mice to a daily dose of UVB radiation. First, the MTD was determined by exposing mice to various doses of UVB, ranging from 500 to 1,250 J/m^2, during seven subsequent days. MTDs of all *p53* defective mouse strains were not different from wild-type K14*cre* mice on a SHK1 hairless background (i.e., in between 750 and 1,000 J/m^2). The presence of a R270H mutation in *p53* and/or a deletion of one or two *p53* alleles apparently do not result in an altered acute sensitivity of the skin to UVB irradiation. Skin tumor-free survivals were determined after a daily dose of 600 J/m^2 UVB and are shown in Fig. 3*A*. Clearly, K14*cre;p53*$^{LSL\text{-}R270H/+}$ mice were much more skin tumor prone than K14*cre;p53*$^{+/+}$ mice ($P < 0.0001$, Fig. 3*B*), indicating that the p53.R270H mutant plays an important role in initiation of UVB-induced skin carcinogenesis. Interestingly, and in contrast to spontaneous skin tumor development, tumor latency times of K14*cre;p53*$^{LSL\text{-}R270H/+}$ mice after UVB exposure were

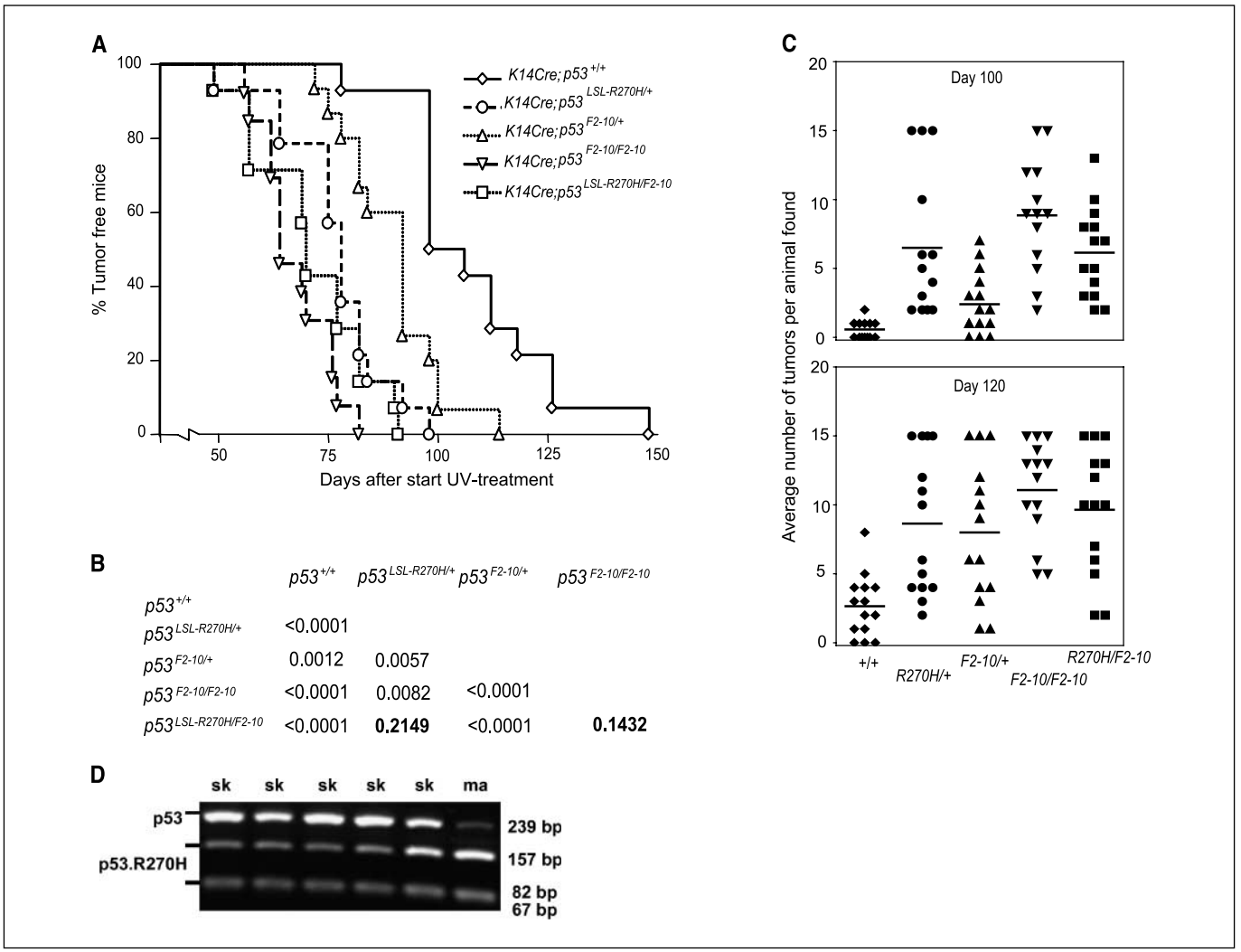

Figure 3. UVB-induced skin tumor development in *p53*-defective K14*cre* mice. Effect of expression of the R270H mutation and/or deletion of exons 2 to 10 in *p53* on UV-induced skin tumor development in *p53*-defective K14*cre* mice. *A,* tumor-free survival curves of K14*cre;p53*$^{+/+}$, K14*cre;p53*$^{LSL\text{-}R270H/+}$, K14*cre;p53*$^{F2\text{-}10/+}$, K14*cre;p53*$^{F2\text{-}10/F2\text{-}10}$, and K14*cre;p53*$^{LSL\text{-}R270H/F2\text{-}10}$ mice in a hairless background after chronic UVB exposure of 600 J/m^2. Time is depicted as days after start of UV treatment. *B,* schematic overview of *P* values of the statistical analyses of UVB-induced tumor-free survival curves analyzed by calculation of Kaplan-Meier distributions of survival and comparison by a two-sided log-rank test. With a level of significance of $P \leq 0.05$, the skin tumor latency time of K14*cre;p53*$^{LSL\text{-}R270H/+}$ mice is significantly different from that observed in K14*cre;p53*$^{F2\text{-}10/+}$ mice, pointing to a dominant-negative effect of the R270H mutant protein. *C,* multiplicity of tumors in the five different genotypes measured at 100 and 120 d after start of the UVB exposure. Total numbers of tumors per individual animals are shown with the mean of the group as horizontal line. Mice with ≥15 tumors were withdrawn from the experiment. Multiplicity of tumors at day 100 is statistically different between K14*cre;p53*$^{LSL\text{-}R270H/+}$ and K14*cre;p53*$^{F2\text{-}10/+}$ mice ($P = 0.0114$, unpaired *t* test) but not between K14*cre;p53*$^{LSL\text{-}R270H/F2\text{-}10}$ and K14*cre;p53*$^{F2\text{-}10/F2\text{-}10}$ mice ($P = 0.1399$, unpaired *t* test). *D,* LOH analysis of UVB-induced skin tumors in K14*cre;p53*$^{LSL\text{-}R270H/+}$ mice by RT-PCR. *Lanes 1* to *5,* clear expression of the wild-type *p53* allele (as well as *p53.R270H* mutant allele) is visible in all skin tumors shown. *Lane 6,* control mammary tumor with 46% LOH from a previous described study in *WAPcre;p53*$^{LSL\text{-}R270H/+}$ mice (25).

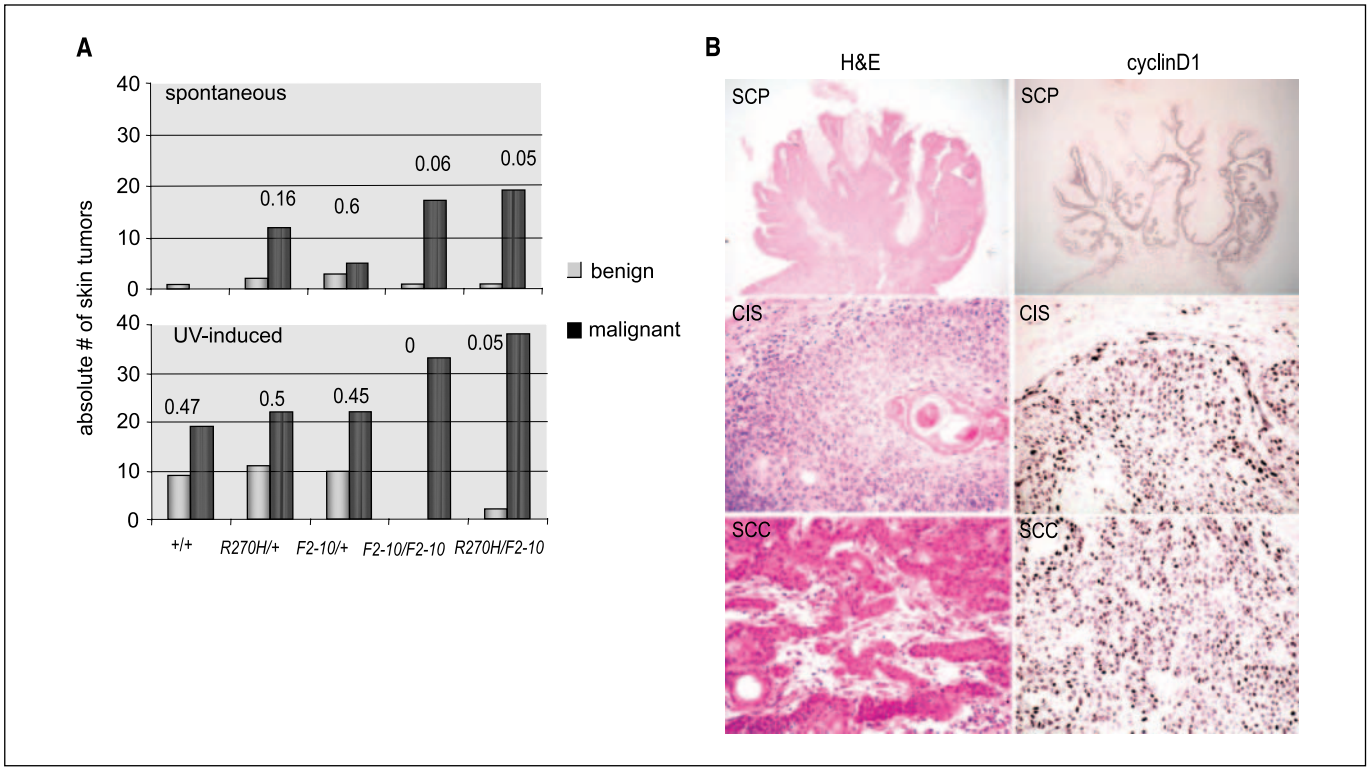

Figure 4. Histologic characterization of skin lesions in *p53*-defective K14*cre* mice. Type of skin lesions in K14*cre;p53*$^{+/+}$, K14*cre;p53*$^{LSL\text{-}R270H/+}$, K14*cre;p53*$^{F2\text{-}10/+}$, K14*cre;p53*$^{F2\text{-}10/F2\text{-}10}$, and K14*cre;p53*$^{LSL\text{-}R270H/F2\text{-}10}$ mice in a hairless background. *A,* schematic graph of the absolute numbers of benign (*light gray columns*) versus malignant (*black columns*) tumors, found either spontaneously or after chronic UVB exposure of 600 J/m^2. The number of benign tumors is taken as the sum of squamous cell papillomas (*SCP*) and keratoacanthoma. The number of malignant tumors is the sum of CIS, SCC, and basal cell carcinoma. Ratios of benign versus malignant tumors are given and used as a determinant for tumor progression. *B,* examples of skin tumor types found (H&E stainings, *left*): SCP of a K14*cre;p53*$^{+/+}$ mouse, CIS and SCC of K14*cre;p53*$^{LSL\text{-}R270H/F2\text{-}10}$ mice, which were all cyclin D1 positive after SP4 staining (*right*). Objectives used are ×2.5 for SCP and ×20 for CIS and SCC.

significantly reduced compared with those in K14*cre;p53*$^{F2\text{-}10/+}$ mice (P = 0.0057), pointing to a dominant-negative effect of the *p53.R270H* mutation. Again, a *p53* gene dose effect was evidently present, as skin tumors developed significantly faster in homozygous K14*cre;p53*$^{F2\text{-}10/F2\text{-}10}$ mice compared with heterozygous K14*cre;p53*$^{F2\text{-}10/+}$ mice (P < 0.0001). Consistent with the spontaneous tumor data, no gain-of-function effect of the *p53.R270H* mutation was detectable on tumor latency in skin epithelium after UVB irradiation.

The presence of a dominant-negative but absence of a gain-of-function effect of the *p53.R270H* mutation on UV-induced latency times was also reflected in multiplicity of UVB-induced skin tumors. Figure 3*C* shows the observed number of skin tumors after 100 and 120 days of UVB exposure. The average number of skin tumors per mouse at day 100 was 6.5 ± 1.4 in K14*cre;p53*$^{LSL\text{-}R270H/+}$ mice, with only 0.6 ± 0.2 tumors developed in wild-type mice during the same time period. Furthermore, a lower number of tumors was observed in K14*cre;p53*$^{F2\text{-}10/+}$ mice (2.4 ± 0.6) compared with K14*cre;p53*$^{LSL\text{-}R270H/+}$ mice. In contrast, tumor multiplicity in homozygous K14*cre;p53*$^{F2\text{-}10/F2\text{-}10}$ mice was similar to that in K14*cre;p53*$^{LSL\text{-}R270H/F2\text{-}10}$ mice. The number of tumors per animal increased over time in all genotypes analyzed and, although smaller, differences in tumor multiplicity between genotypes were also detectable after 120 days of UVB exposure (Fig. 3*C*).

Molecular analysis of UVB-induced skin tumors. To verify the observed dominant-negative effect of the *p53.R270H* mutation on skin tumor latency as well as tumor multiplicity on the molecular level, a representative nonselective subset of 11 tumors from 11 individual K14*cre;p53*$^{LSL\text{-}R270H/+}$ mice was analyzed for LOH by RT-PCR analysis. No LOH was observed in any of the analyzed UVB-induced skin tumors (Fig. 3*D*), indicating that loss of the wild-type *p53* allele was not advantageous for tumor formation.

It is known that during later phases of UV-induced skin tumor development in both humans and mice, p53 function can be (further) altered by acquired gene mutations (32, 35–40). We investigated therefore whether the development of UV-induced skin tumors in K14*cre;p53*$^{LSL\text{-}R270H/+}$ mice was solely the result of the initial *p53.R270H* mutation, or whether it was accompanied by the formation of additional *p53* mutations. For this, we analyzed at random 17 skin tumors from 16 individual K14*cre;p53*$^{LSL\text{-}R270H/+}$ mice by direct exon sequencing of the *p53* gene. The majority of tumors (14 of 17) contained one or more additional *p53* mutations (Supplementary Table S1).

Histologic characterization of skin tumors. Spontaneous and UV-induced skin lesions were analyzed for histologic characteristics. Both groups of mice developed epithelial, proliferative lesions forming a continuum from nonneoplastic squamous keratosis and acanthosis to squamous cell papillomas (SCP), actinic keratosis, and keratoacanthoma with increasing degrees of atypia and dysplasia, carcinoma *in situ* (CIS), up to invasive SCC (Fig. 4). Basal cell carcinomas were also found in unexposed mice with deleted *p53* alleles, but not in mice with a *p53.R270H* mutation or after UV exposure. There seems to be a trend towards more spontaneous carcinomas in K14*cre;p53*$^{LSL\text{-}R270H/+}$ mice when

compared with mice with a heterozygous deletion of *p53*, with an incidence of carcinomas almost similar to that found in K14*cre;p53*$^{F2\text{-}10/F2\text{-}10}$ and K14*cre;p53*$^{LSL\text{-}R270H/F2\text{-}10}$ mice (Fig. 4*A*).

The majority of proliferative lesions after UVB in all genotypes were classified as actinic keratosis, representing premalignant precursors of SCC. No gross differences in UV-induced actinic keratosis numbers were detectable between the five genotypes analyzed (data not shown). For determination of tumor progression status, the ratios between benign versus malignant skin tumors was calculated. Calculated ratios were 0.47, 0.5, and 0.45 for K14*cre;p53*$^{+/+}$, K14*cre;p53*$^{LSL\text{-}R270H/+}$, and K14*cre;p53*$^{F2\text{-}10/+}$ mice, respectively, indicating that although inactivation of one *p53* allele in skin epithelium has an influence on time of onset of UV-induced tumors (see Fig. 3*A*), no effect was observed on tumor progression to a malignant state. Furthermore, no dominant-negative effect of p53.R270H mutant protein could be observed on skin tumor progression. Interestingly, strongly accelerated tumor progression was observed in mice with homozygous *p53* inactivation, as already reported previously for UV-exposed conventional $p53^{-/-}$ mice (35). The ratio benign versus malignant tumors was very low in K14*cre;p53*$^{F2\text{-}10/F2\text{-}10}$ as well as K14*cre;p53*$^{LSL\text{-}R270H/F2\text{-}10}$ mice ($\leq$0.05), indicating that loss of the second *p53* allele has dramatic effects on tumor progression.

A *p53* gain-of-function effect has been described to be accompanied by overexpression of oncogenes (12). To investigate possible gain-of-function effects of the *p53.R270H* mutation in skin tumor development, sections of UV-induced skin tumors were stained with antibodies against *cyclin D1* and *H-Ras*, which are both associated with skin tumor development in mice and men (41, 42). Figure 4*B* shows a representative panel of tumors stained for H&E and cyclin D1. Prominent cyclin D1 expression was visible in all UV-induced skin tumors tested, varying from SCP to SCC. However, no differences could be observed between tumors developed in the various *p53*-defective genotypes (data not shown), pointing to the absence of a gain-of-function effect. The same results were obtained for H-Ras: clear expression was visible in UV-induced skin tumors without genotypic differences (data not shown).

Analysis of sunburn cells after short-term UVB exposure. Inactive *p53* in mouse skin has been reported to reduce the appearance of sunburn cells (apoptotic keratinocytes generated by overexposure to UV), and as such, the loss of *p53* provides a survival advantage to UV-damaged cells (43). To identify potential dominant-negative effects of the *p53.R270H* mutation on apoptosis in an early stage, we analyzed skin samples of the five different *p53*-defective genotypes for the presence of apoptotic cells after short-term UVB exposure using H&E and caspase-3 staining. In addition, the UVB-exposed skin sections were stained for different known *p53* targets involved in apoptosis, with Bax and Puma representing the mitochondrial intrinsic pathway and Perp representing the cell membrane extrinsic pathway (44). Figure 5*A* shows that the highest amount of caspase-3–positive cells are found in K14*cre;p53*$^{+/+}$ skin exposed to a single dose of 500 J/m^2 UVB, and all UV-exposed skin samples of *p53*-defective mice showed a significant decrease in caspase-3–positive cells. However, hardly any difference could be observed between K14*cre;p53*$^{LSL\text{-}R270H/+}$, K14*cre;p53*$^{F2\text{-}10H/+}$, or K14*cre;p53*$^{F2\text{-}10H/F2\text{-}10}$ mice (Fig. 5*A*). In line with this, the amount of sunburn cells after a single exposure to UVB, counted in H&E sections, was increasing with dose, with the highest amount in K14*cre;p53*$^{+/+}$ skin and decreased numbers of sunburn cells in all *p53*-defective genotypes (data not shown). Figure 5*B* shows examples of Bax stainings of K14*cre;p53*$^{+/+}$, K14*cre;p53*$^{LSL\text{-}R270H/+}$, and

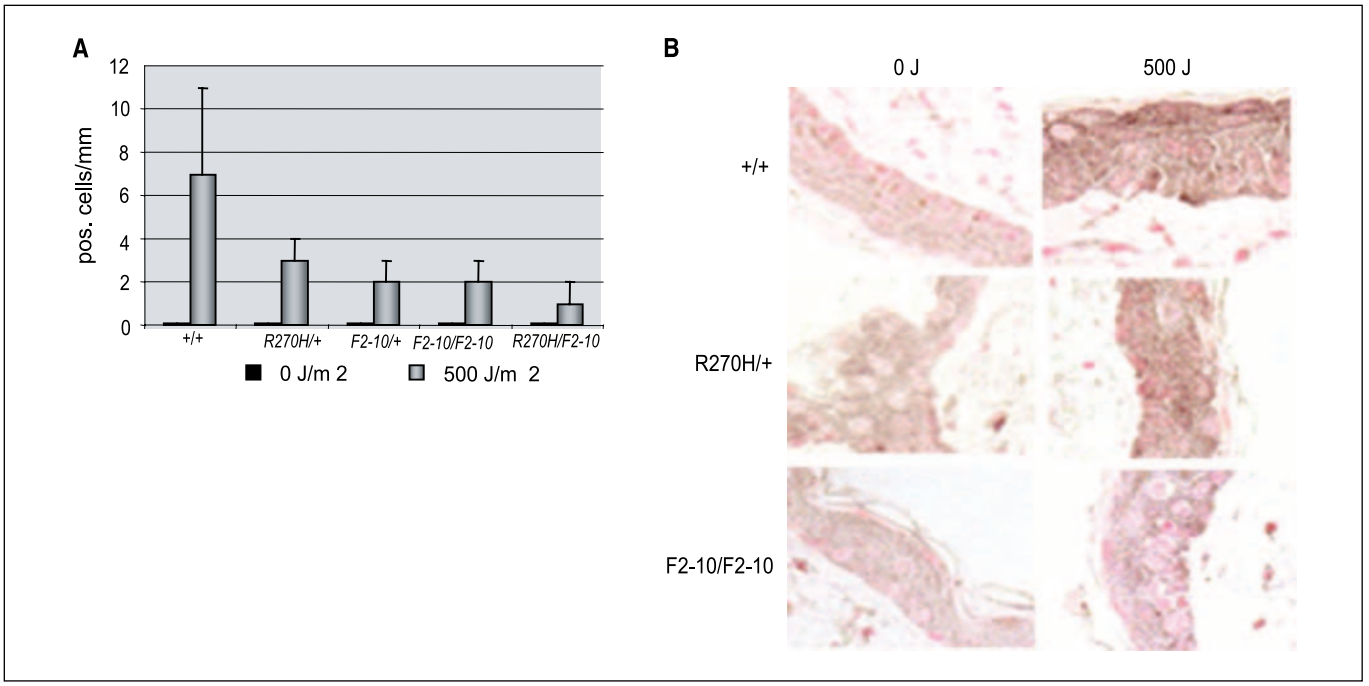

Figure 5. Analysis of apoptotic cells and expression of Bax after short-term UVB exposure in *p53*-defective K14*cre* mice. *A,* number of caspase-3–positive cells per mm in either untreated or UVB-exposed skin sections of K14*cre;p53*$^{+/+}$, K14*cre;p53*$^{LSL\text{-}R270H/+}$, K14*cre;p53*$^{F2\text{-}10/+}$, K14*cre;p53*$^{F2\text{-}10/F2\text{-}10}$, and K14*cre;p53*$^{LSL\text{-}R270H/F2\text{-}10}$ mice in a hairless background. Caspase-3 is one of the key executioners of apoptosis as it is either partially or totally responsible for the proteolytic cleavage of many proteins such as poly(ADP-ribose) polymerase (45). *B,* Bax stainings of K14*cre;p53*$^{+/+}$, K14*cre;p53*$^{LSL\text{-}R270H/+}$, and K14*cre;p53*$^{F2\text{-}10/F2\text{-}10}$ skin, untreated (*left*) or after 500 J/m^2 UVB (*right*).

K14*cre;p53*$^{F2\text{-}10/F2\text{-}10}$ skin. No detectable expression of the Bax protein was observed in unexposed skin, whereas UV exposure resulted in a slight increase in Bax-positive cells in wild-type skins. The number of Bax-positive cells was decreased in *p53*-defective skin compared with K14*cre;p53*$^{+/+}$ skin, with similar staining patterns in skins of K14*cre;p53*$^{LSL\text{-}R270H/+}$ and K14*cre;p53*$^{F2\text{-}10/+}$ mice. Homozygous inactivation of *p53* in skin resulted in a slightly lower amount of Bax-positive cells than heterozygous inactivation. Similar results were obtained for staining against Perp (data not shown).

Discussion

In the present study, we have investigated potential dominant-negative and/or gain-of-function effects of a *p53.R270H* mutation, equivalent to the human hotspot R273H mutation, on development and progression of mouse skin tumors. For this, conditional mutant *p53*$^{LSL\text{-}R270H}$ mice (22) were crossed with K14*cre* mice (31), resulting in physiologic expression levels of the mutant p53.R270H protein in skin epithelium. This analysis was done for skin tumors that arose spontaneously as well as after the induction of DNA damage, because one could hypothesize inhibitory or oncogenic effects of mutant p53 might be more abundant following p53 activation by DNA damage. Because we used as controls conditional K14*cre;p53*$^{F2\text{-}10}$ knockout mice on a similar hairless background as the K14*cre;p53*$^{LSL\text{-}R270H}$ mice, a clean comparison could be made between deletion and mutation of *p53* in skin without early occurrence of lymphomas or sarcomas. Lethality caused by these non-epithelial tumors has hampered analysis of UV-induced skin tumor formation in conventional *p53*-null mice up to now (35, 45).

Our data indicate absence of dominant-negative and gain-of-function effects of the R270H mutation on spontaneous skin tumor development, because (*a*) heterozygous K14*cre;p53*$^{LSL\text{-}R270H/+}$ mice do not show accelerated tumor development compared with heterozygous K14*cre;p53*$^{F2\text{-}10/+}$ mice, and because (*b*) homozygous K14*cre;p53*$^{F2\text{-}10/F2\text{-}10}$ and K14*cre;p53*$^{LSL\text{-}R270H/F2\text{-}10}$ mice develop tumors with similar latencies. These results suggest that expression of mutant p53.R270H in skin epithelium does not interfere with the function of wild-type p53 and, furthermore, does not have novel oncogenic functions, at least not with respect to tumor latency. These findings are in contrast to previous results found in mammary epithelium (25) and lung epithelium (26), where a spontaneous dominant-negative phenotype of the p53.R270H protein was found, indicating that dominant-negative properties are tissue specific and/or dependent of p53 expression levels.

Although we have not detected dominant-negative and gain-of-function effects of p53.R270H on the latency of spontaneous skin tumors, histopathologic examination revealed a small change in tumor spectrum (Fig. 4*A*). K14*cre;p53*$^{LSL\text{-}R270H/+}$ mice spontaneously develop slightly more carcinomas compared with K14*cre;p53*$^{F2\text{-}10/+}$ mice, suggesting a possible dominant-negative effect of the *p53.R270H* mutation on tumor progression. Although the absolute numbers of tumors analyzed are too low to draw firm conclusions, this increase in carcinoma development is in line with previous results in *p53*$^{R270H/+}$ mice, which showed a significantly higher incidence of carcinomas in lung, liver, kidney, intestine, and skin compared with conventional *p53*$^{+/-}$ mice (22). However, the additional gain-of-function effect observed in *p53*$^{R270H/-}$ mice (which develop more carcinomas than conventional *p53*$^{-/-}$ mice) is absent in our skin-specific *p53* mouse mutants, because no difference in skin tumor progression could be observed between K14*cre;p53*$^{LSL\text{-}R270H/-}$ and K14*cre;p53*$^{F2\text{-}10/F2\text{-}10}$ mice. An explanation for this could lie in the fact that the conventional *p53*$^{-/-}$ mice used in earlier studies did not develop carcinomas at all (22), likely due to early death from lymphomas. This clearly shows the importance of using tissue-specific mouse mutants for genotype-phenotype correlation studies.

Here, in a SKH-1 background, mammary tumors were only found in K14*cre;p53*$^{LSL\text{-}R270H/+}$ mice, whereas in a recently conducted study in a FVB background, also K14*cre;p53*$^{F2\text{-}10/F2\text{-}10}$ mice developed mammary tumors at high incidence.[5] Genetic background differences are probably causing this apparent discrepancy.

Interestingly, effects of the presence of one mutant *p53.R270H* allele after the induction of DNA damage are very different from those observed spontaneously. Chronic *in vivo* UV exposure leads to the development of a broad pattern of skin tumors in mice of all *p53* genotypes. In contrast to the spontaneous tumor development study, a clear dominant-negative effect of the *p53.R270H* mutation on both latency and multiplicity of UV-induced skin tumors was detected. Apparently, the expression levels of mutant *p53* are crucial for manifestation of dominant-negative activity during skin tumor formation. These findings are corroborated by previous results from these *p53* point mutant mice (21, 22), where accumulation of mutant p53 was found following induction of DNA damage in homozygous mutant MEFs. In addition, the dominant-negative activity of mutant p53 increased after DNA damage in various tissues of heterozygous mutant mice (21, 22). We have found similar stabilization of mutant p53.R270H in the skin after short-term UVB exposure (data not shown). It is well known that upon induction of DNA damage, wild-type p53 protein accumulates and stabilizes, resulting in transactivation of target genes protecting the genome by a variety of cellular responses (2). Apparently, to uncover its dominant-negative or gain-of-function characteristics, mutant p53 also needs to accumulate and be stabilized, presumably through mechanisms similar to that of wild-type p53 (46). Stabilization of mutant p53 may strongly inhibit tumor suppressive functions of wild-type p53 and as such account for the observation that K14*cre;p53*$^{LSL\text{-}R270H/+}$ mice display a more severe tumor phenotype than K14*cre;p53*$^{F2\text{-}10/+}$ mice after exposure to UVB. However, due to the construction of the K14*cre;p53*$^{LSL\text{-}R270H}$ mouse model, cells surrounding the tumor are *p53*$^{+/-}$, whereas these are *p53*$^{+/+}$ in K14*cre;p53*$^{F2\text{-}10}$ mice. A supporting effect of the surrounding cells on tumor development can therefore not be excluded.

The accelerated skin tumor development in K14*cre;p53*$^{LSL\text{-}R270H/+}$ mice was a clear dominant-negative effect of the mutation, because no loss of the wild-type *p53* allele was found in these tumors. The absence of LOH was not entirely unexpected, because also previous studies showed that LOH was a rare event in UV-induced skin tumors of *p53*$^{+/-}$ mice (35, 36, 43, 47, 48). However, in the majority of skin tumors analyzed, we identified one or more additional *p53* mutations in codons described before for various *p53*-defective mice exposed to UV (32, 47). It remains yet to be determined whether these additional mutations inactivate the wild-type allele and are critical for skin tumor formation, because

[5] X. Liu et al. Somatic loss of BRCA1 and p53 in mice induces mammary tumors with pathologic and molecular features of human *BRCA1*-mutated basal-like breast cancer, submitted for publication.

it might well be that these mutations are formed during the process of tumor development when genome instability is a well-known characteristic.

Dominant-negative effects of p53.R270H protein could not be shown in progression of skin tumors after UVB exposure, because the same fraction of malignant tumors was found in heterozygous point mutants, heterozygous conditional knockouts, and even wild-type p53 mice (Fig. 4*A*). Maybe the load of UV-induced DNA damage was too high to find subtle differences in tumor progression at the time of tumor isolation. We used tumor size and multiplicity as an end point in our experiments (i.e., tumors $\geq$ 4 mm or $\geq$15 small tumors). For detection of subtle differences, it might be better to analyze tumor progression at fixed time points after start of UV exposure, as was done for determining multiplicity of tumors. Only mutation or deletion of both *p53* alleles resulted in significantly more malignant CIS and SCC, most likely because total absence of p53 results in loss of cell cycle checkpoints, impaired DNA damage responses, and apoptotic resistance (43).

Tumor-associated p53 mutant proteins can exert gain-of-function activity via inhibition of p53-independent apoptosis as well as through activation of oncogenes (8). Overexpression of cyclin D1 has been found in (early stages of) many tumors, including mouse and human skin tumors (41, 42). Furthermore, the expression of cyclin D1 is related to sun exposure (41). Several studies also show a correlation between cyclin D1 expression levels and Ras activation. Cyclin D1 is a critical target of oncogenic Ras in mouse skin carcinogenesis and has a role as a downstream mediator of Ras activity during tumor development (42). Therefore, protein levels of these two oncogenes were determined in skin tumors from mice of all p53 genotypes, to identify potential gain-of-function effects of p53.R270H on oncogene expression in skin tumor development. Lack of gain-of-function properties was suggested by similar patterns of cyclin D1 and H-Ras staining in UV-induced skin tumors of mice of all genotypes, including $p53^{R270H/F2\text{-}10}$ and $p53^{F2\text{-}10/F2\text{-}10}$. Apparently, protein levels of skin tumor–related oncogenes are not directly increased by the presence of p53.R270H mutant protein, at least not the well-known examples analyzed here.

The dominant-negative effect of p53.R270H on UVB-induced tumor induction could not be clearly shown in the early apoptotic response after short-term UVB exposure. Although the number of apoptotic cells was decreased dramatically compared with wild-type responses, no differences were observed between K14*cre;*$p53^{LSL\text{-}R270H/+}$ and K14*cre;*$p53^{F2\text{-}10/+}$ mice in apoptotic cell numbers and expression of known p53 targets involved in different apoptotic pathways. Apparently, the selection of cells resistant against apoptosis in an early stage is not the only crucial factor in initiation and development of UVB-induced skin tumors. A decreased ability of damaged cells to undergo cell cycle arrest, or the induction of mutations in preneoplastic lesions, might also strongly influence tumor development.

In conclusion, our studies show that p53.R270H mutant protein has dominant-negative but not gain-of-function properties in skin epithelium. More specifically, dominant-negative features of mutant p53 protein in skin epithelium are exclusively apparent after the induction of DNA damage. Whether these DNA damage–related differences in mutant p53 characteristics are also found in other tissues and/or after exposure to other DNA-damaging compounds is an interesting question that remains to be addressed.

Acknowledgments

Received 12/20/2006; revised 2/16/2007; accepted 2/26/2007.

Grant support: Dutch Cancer Society grant KWF 2000-2352 and NIH/National Institute of Environmental Health Sciences, Comparative Mouse Genomics Centers Consortium grant 1UO1 ES11044-02.

The costs of publication of this article were defrayed in part by the payment of page charges. This article must therefore be hereby marked *advertisement* in accordance with 18 U.S.C. Section 1734 solely to indicate this fact.

We thank the Central Animal Facility Laboratory (NVI-GPL) for their skillful (bio)technical support.

References

1. Vogelstein B, Lane D, Levine AJ. Surfing the p53 network. Nature 2000;408:307–10.
2. Prives C, Hall PA. The p53 pathway. J Pathol 1999;187:112–26.
3. Malkin DD, Li FP, Strong LC, et al. Germ line p53 mutations in a familial syndrome of breast cancer, sarcomas, and other neoplasms. Science 1990;250:1233–8.
4. Srivastava S, Zou ZQ, Pirollo K, Blattner W, Chang EH. Germ-line transmission of a mutated p53 gene in a cancer-prone family with Li-Fraumeni syndrome. Nature 1990;348:747–9.
5. Bartek J, Bartkova J, Vojtesek B, et al. Aberrant expression of the p53 oncoprotein is a common feature of a wide spectrum of human malignancies. Oncogene 1991;6:1699–703.
6. Greenblatt MS, Bennet WP, Hollstein M, Harris CC. Mutations in the p53 tumor suppressor gene: clues to cancer etiology and molecular pathogenesis. Cancer Res 1994;54:4855–78.
7. Levine AJ. The tumor suppressor genes. Annu Rev Biochem 1993;62:623–51.
8. Sigal A, Rotter V. Oncogenic mutations of the p53 suppressor: the demons of the guardian of the genome. Cancer Res 2000;60:6788–93.
9. Bullock AN, Fersht AR. Rescuing the function of mutant p53. Nat Rev Cancer 2001;1:68–76.
10. Koonin EV, Rogozin IB, Glazko GV. p53 Gain of function, Tumor biology and bioinformatics come together. Cell Cycle 2005;4:686–8.
11. Milner J, Medcalf EA, Cook AC. Tumor suppressor p53: analysis of wild-type and mutant p53 complexes. Mol Cell Biol 1991;11:12–9.
12. Dittmer D, Pati S, Zambetti G, et al. Gain of function mutations in p53. Nat Genet 1993;4:42–5.
13. Donehower LA. The p53 deficient mouse: a model for basic and applied cancer studies. Semin Cancer Biol 1996;7:269–78.
14. Attardi LD, Jacks T. The role of p53 in tumour suppression: lessons from mouse models. Cell Mol Life Sci 1999;22:48–63.
15. Attardi LD, Donehower LA. Probing p53 biological functions through the use of genetically engineered mouse models. Mutat Res 2005;576:4–21.
16. Harvey M, Vogel H, Morris D, Bradley A, Bernstein A, Donehower L. A mutant p53 transgene accelerates tumour development in heterozygous but not nulligous p53-deficient mice. Nat Genet 1995;9:305–11.
17. Lavigueur A, Maltby V, Mock D, Rossant J, Pawson T, Bernstein A. High incidence of lung, bone, and lymphoid tumors in transgenic mice overexpressing mutant alleles of the p53 oncogene. Mol Cell Biol 1989;9:3982–91.
18. Li B, Murphy KL, Laucirica R, Kittrell F, Medina D, Rosen JM. A transgenic mouse model for mammary carcinogenesis. Oncogene 1998;16:997–1007.
19. Wang XJ, Greenhalgh DA, Jiang A, et al. Expression of a p53 mutant in the epidermis of transgenic mice accelerates chemical carcinogenesis. Oncogene 1998;17:35–45.
20. Duan W, Ding H, Subler MA, et al. Lung-specific expression of human mutant p53–273H is associated with a high frequency of lung adenocarcinoma in transgenic mice. Oncogene 2002;21:7831–8.
21. Lang GA, Iwakuma T, Suh Y-A, et al. Gain of function of a p53 hot spot mutation in a mouse model of Li-Fraumeni syndrome. Cell 2005;119:861–72.
22. Olive KP, Tuveson DA, Ruhe ZC, et al. Mutant p53 gain of function in two mouse models of Li Fraumeni syndrome. Cell 2004;119:847–60.
23. Hollstein M, Sidransky D, Vogelstein B, Harris CC. p53 mutations in human cancers. Science 1991;253:49–53.
24. Hamroun D, Kato S, Ishioka C, Claustres M, Beroud C, Soussi T. The UMD TP53 database and website: update and revisions. Hum Mutat 2006;27:14–20.
25. Wijnhoven SWP, Zwart E, Speksnijder EN, et al. Mice expressing a mammary gland-specific R270H mutation in the p53 tumor suppressor gene mimic human breast cancer development. Cancer Res 2005;65:8166–72.
26. Jackson EL, Olive KP, Tuveson DA, et al. The differential effects of mutant p53 alleles on advanced murine lung cancer. Cancer Res 2005;65:10280–8.
27. Bowden GT. Prevention of non-melanoma skin cancer by targeting ultraviolet-B-light signaling. Nat Rev Cancer 2004;4:23–35.
28. Decraene D, Agostinis P, Pupe A, De Haes P, Garmyn M. Acute response of human skin to solar radiation;

regulation and function of the p53 protein. J Photochem Photobiol 2001;B63:78–83.
29. Venkatachalam S, Shi Y-P, Jones SN, et al. Retention of wild-type p53 in tumors form p53 heterozygous mice: reduction of p53 dosage promote cancer formation. EMBO J 1998;17:4657–67.
30. De Vries A, Flores ER, Miranda B, et al. Targeted point mutations of p53 lead to dominant-negative inhibition of wild-type p53 function. Proc Natl Acad Sci U S A 2002;99:2948–53.
31. Jonkers J, Meuwissen R, Van der Gulden H, Peterse H, Van der Valk M, Berns A. Synergistic tumor suppressor activity of BRCA2 and p53 in a conditional mouse model for breast cancer. Nat Genet 2001;29:418–25.
32. Hoogervorst EM, Bruins W, Zwart E, et al. Lack of p53 Ser389 phosphorylation predisposes mice to develop 2-acetylaminofluorene-induced bladder tumors but not ionizing radiation-induced lymphomas. Cancer Res 2005;65:3610–6.
33. Ihrie RA, Marques MR, Nguyen BT, et al. Perp is a p63-regulated gene essential for epithelial integrity. Cell 2005;120:843–56.
34. Hoogervorst EM, Van Oostrom CThM, Beems RB, et al. p53 heterozygosity results in an increased 2-acetylaminofluorene-induced urinary bladder but not liver tumor response in DNA repair-deficient Xpa mice. Cancer Res 2004;64:5118–26.
35. Jiang W, Ananthaswamy HN, Muller HK, Kripke ML. p53 protects against skin cancer induction by UV-B radiation. Oncogene 1999;18:4247–53.
36. Dumaz N, Van Kranen HJ, De Vries A, et al. The role of UVB-light in skin carcinogenesis through the analysis of p53 mutations in squamous cell carcinomas of hairless mice. Carcinogenesis 1997;18:897–904.
37. Kress S, Sutter C, Strickland PT, Mukhtar H, Schweizer J, Schwarz M. Carcinogen-specific mutational pattern in the p53 gene in ultraviolet B radiation-induced squamous cell carcinomas of mouse skin. Cancer Res 1992;52:6400–3.
38. Reis AM, Cheo DL, Meira LB, et al. Genotype-specific Trp53 mutational analysis in ultraviolet B radiation-induced skin cancers in Xpc and Xpc Trp53 mutant mice. Cancer Res 2000;60:1571–9.
39. Kanjilal S, Pierceall WE, Cummings KK, Kripke ML, Anathaswamy HN. High frequency of p53 mutations in ultraviolet radiation-induced murine skin tumors: evidence for strand bias and tumor heterogeneity. Cancer Res 1993;53:2961–4.
40. Van Kranen HJ, de Gruijl FR, de Vries A, et al. Frequent p53 alterations but low incidence of ras mutations in UV-B-induced skin tumors of hairless mice. Carcinogenesis 1995;5:1141–7.
41. Liang S-B, Furihata M, Takeuchi T, et al. Over-expression of cyclin D1 in nonmelanocytic skin cancer. Virchows Arch 2000;436:370–6.
42. Rodriguez-Puebla ML, Robles AI, Conti CJ. Ras activity and cyclin D expression: an essential mechanism of mouse skin tumor development. Mol Carcinog 1999;24:1–6.
43. Ziegler A, Jonason AS, Leffell DJ, et al. Sunburn and p53 in the onset of skin cancer. Nature 1994;372:773–6.
44. Haupt S, Berger M, Goldberg Z, Haupt Y. Apoptosis: the p53 network. J Cell Sci 2003;116:4077–85.
45. Fernandez-Alnemri T, Litwach G, Alnemri ES. CPP32, a novel human apoptotic protein with homology to *Caenorhabditis elegans* cell death protein Ced-3 and mammalian interleukin 1β-converting enzyme. J Biol Chem 1994;269:30761–4.
46. Iwakuma T, Lozano G, Flores ER. Li-Fraumeni syndrome, a p53 family affair. Cell Cycle 2005;4:865–7.
47. Van Kranen HJ, Westerman A, Berg RJW, et al. Dose-dependent effects of UVB- induced skin carcinogenesis in hairless p53 knockout mice. Mutat Res 2005;571:81–90.
48. Ziegler A, Leffell DJ, Kunala S, et al. Mutation hotspots due to sunlight in the p53 gene of nonmelanoma skin cancers. Proc Natl Acad Sci U S A 1993;90:4216–20.

Dominant-Negative but not Gain-of-Function Effects of a *p53.R270H* Mutation in Mouse Epithelium Tissue after DNA Damage

Susan W.P. Wijnhoven, Ewoud N. Speksnijder, Xiaoling Liu, et al.

Cancer Res 2007;67:4648-4656.